

---

# A Generation Framework with Strict Constraints for Crystal Materials Design

---

Chao Huang<sup>1,2,3\*</sup> Jiahui Chen<sup>2†</sup> Chen Chen<sup>2†</sup> Chunyan Chen<sup>2</sup> Renjie Su<sup>2,5</sup>  
Shiyu Du<sup>4</sup> ChenChen<sup>2</sup> Hongrui Liang<sup>2,6</sup> Daojing Lin<sup>2</sup>

<sup>1</sup>Institute of Computing Technology, Chinese Academy of Science, Beijing, China

<sup>2</sup>Ningbo Institute of Artificial Intelligence Industry, Ningbo, China

<sup>3</sup>Hangzhou Institute for Advanced Study, UCAS, Hangzhou, China

<sup>4</sup>China University of Petroleum (East China), Qingdao, China

<sup>5</sup>Ningbo Institute of Materials Technology and Engineering, CAS, Ningbo, China

<sup>6</sup>Polytechnic Institute, Zhejiang University, Hangzhou, China  
chuang@ict.ac.cn

## Abstract

The design of crystal materials plays a critical role in areas such as new energy development, biomedical engineering, and semiconductors. Recent advances in data-driven methods have enabled the generation of diverse crystal structures. However, most existing approaches still rely on random sampling without strict constraints, requiring multiple post-processing steps to identify stable candidates with the desired physical and chemical properties. In this work, we present a new constrained generation framework that takes multiple constraints as input and enables the generation of crystal structures with specific chemical and properties. In this framework, intermediate constraints, such as symmetry information and composition ratio, are generated by a constraint generator based on large language models (LLMs), which considers the target properties. These constraints are then used by a subsequent crystal structure generator to ensure that the structure generation process is under control. Our method generates crystal structures with a probability of meeting the target properties that is more than twice that of existing approaches. Furthermore, nearly 100% of the generated crystals strictly adhere to predefined chemical composition, eliminating the risks of supply chain during production.

## 1 Introduction

Designing novel and high-performance crystal structures has long been recognized as a critical research direction in materials science. Traditional crystal materials design relies on computational simulations, such as Density Functional Theory (DFT) (1) and high-throughput calculations, which demand substantial human expertise and computational resources (2). Over the past few decades, the application of computer technology in the field of crystal structure generation has made systematic new materials design a reality (3), leading to the emergence of a series of representative methods, such as simulated annealing (4), random search (5), genetic algorithms (6), and particle swarm optimization (7). Nevertheless, these methods still exhibit limitations in generating valid and diverse crystal structures.

In recent years, large open-source material databases (8; 9; 10) have greatly advanced data-driven methods in crystal generation (11; 12). Among these, generative models have been proved particularly

---

\*Corresponding Author.

†Equal contribution.

effective in generating valid and diverse crystal structures (13; 14). However, constraint-based targeted crystal structure generation has remained challenging. CrystalFormer (15) generates space group-controlled crystal materials using space groups as initial constraint, while DiffCSP++ (16) produces strictly symmetry-compliant crystals based on elemental and symmetry constraints. MatterGen (17) proposes a conditional diffusion model capable of guiding materials generation with specified constraints, including properties and chemical composition, though these constraints remain flexible and do not always fully meet the preset conditions.

In this work, we propose a novel two-step crystal structure generation framework with strict constraints, which we refer as CrystalGF. In the first step, our constraints generation module analyzes the input chemical composition and target material properties, then produces more strict constraints such as symmetry information and component ratios. In the second step, our structure generation module outputs the desired crystal structures conforming to both the original and newly generated constraints. Our contributions can be summarized as follows:

- We design a novel two-step crystal generation framework that only requires chemical composition and material properties as input information. By automatically generating symmetry-related constraints, this framework produces crystals that better satisfy target properties while strictly adhering to prescribed chemical composition.
- We develop a LLMs-based constraint generator that generates the space groups of unit cells, the Wyckoff positions for atoms, and the composition ratio based on specified chemical composition and target material properties. This module provides high-quality priors for the subsequent generation of structures and enables our methods to take input from natural language.
- We design a strict constrained crystal structure generator that operates under joint constraints of chemical composition, target properties, and symmetry requirements. This module ensures strict compliance with all specified constraints during structure generation.
- Compared to prior generative models, structures produced by our method are more than twice as likely to meeting the target properties. More precisely, 66.49% of the generated structures achieved band gap deviations below 0.05 eV and 24.68% exhibited formation energy deviations within 0.05 eV/atom. In addition, nearly 100% of the generated crystals strictly adhere to the initial composition, eliminating supply chain risks during production.

## 2 Related works

**Crystal Structure Generation** Crystal structure generation methods based on data-driven have witnessed rapid advancements. CDVAE (13) combines the variational autoencoder (VAE) with diffusion model, first generating atomic types and lattice vectors from encoded crystal features, and then using these as conditional inputs to the diffusion model to generate new crystal structures. Building upon CDVAE, Con-CDVAE (18) incorporates material properties as conditions for crystal generation and designs a two-step training method to align the encoded features of properties. DiffCSP (14) optimizes the generation of lattice matrices and atomic coordinates through a joint diffusion framework, while its successor DiffCSP++ (16) introduces constraints based on crystal symmetry, using symmetry basis matrices to constrain the lattice vectors and Wyckoff position coordinates to constrain the atomic coordinates, ensuring that the generated crystal structures strictly adhere to the input crystal symmetry. MatterGen (17) adopts a joint diffusion framework, uses polar decomposition to represent the lattice as  $O(3)$ -invariant symmetric matrices, and further introduces an adapter module for fine-tuning based on specific property constraints. UniMat (19) proposes a unified method to represent any crystal structure to address the compression problem of crystal information, and trains a diffusion model on this representation. Compared to the aforementioned methods, our proposed model generates more desirable and accurate crystal structures by incorporating both input and self-generated constraints.

**Crystal Symmetry Generation** Crystal symmetry, encompassing space groups and Wyckoff positions, plays a pivotal role in the description of crystal structures. We demonstrate the effects of symmetry on the lattice geometry and atomic arrangements in Table 5 and Figure 6 respectively. Determining symmetry simplifies the complexity of generating crystal structures. Zhao et al. (20) proposed a neural network model that combined Random Forest (RF) and Multi-Layer Perceptron (MLP), and achieved effective prediction of crystal systems and space groups by incorporating

features such as Magpie, atomic vectors, and one-hot encoding. Wang et al. (21; 22) proposed a space group prediction method based on crystal chemical formulas and crystal-related feature descriptors (such as total atomic count, average atomic radius, maximum sound velocity, minimum polarizability, and other properties). Rewc-GNN (23) aims to predict the space groups of porphyrin crystals by encoding the atomic properties and interatomic interactions within the crystal through the integration of the Rewc algorithm and Graph Neural Networks. Learning-based crystal space group prediction models have demonstrated significant potential in prediction accuracy and generalization capabilities, providing robust support for the discovery and design of novel crystal structures. However, based on our current literature review, research on LLM-based symmetry prediction, and studies focusing on Wyckoff position prediction within crystal symmetry, remains relatively scarce.

**Large Language Models** Over the past few years, LLMs have undergone rapid iteration and evolution (24; 25), gradually approaching and even surpassing human-level performance across various complex benchmarks. Alongside proprietary models, open-source counterparts have achieved remarkable progress, including the DeepSeek series (26; 27), LLaMA series (28; 29), Qwen series (30; 31), and GLM series (32; 33). These open-source models are progressively narrowing the performance gap with their closed-source counterparts. LLMs have also found broad applications in materials science: MatChat (34) generates high-confidence solid-state reaction pathways by analyzing inorganic materials synthesis data from tens of thousands of research papers. The MatterChat (35) model achieves breakthrough capabilities by integrating atomic structural data with natural language processing, bridging machine-learned interatomic potentials with pretrained LLMs to enable full-resolution atomic structure analysis. The LLMatDesign (36) framework leverages LLM agents for zero-shot prediction of material properties and novel materials design. The GPTFF (37) universal pretrained force field, incorporating Transformer attention mechanisms, delivers precise predictions of interatomic interactions. CrystalLLM (38) employs LLMs to generate crystal structures. However, since learning and generating extensive atomic coordinates fall outside the core competencies of LLMs, this paper proposes the development of a crystal constraint generator powered by LLMs.

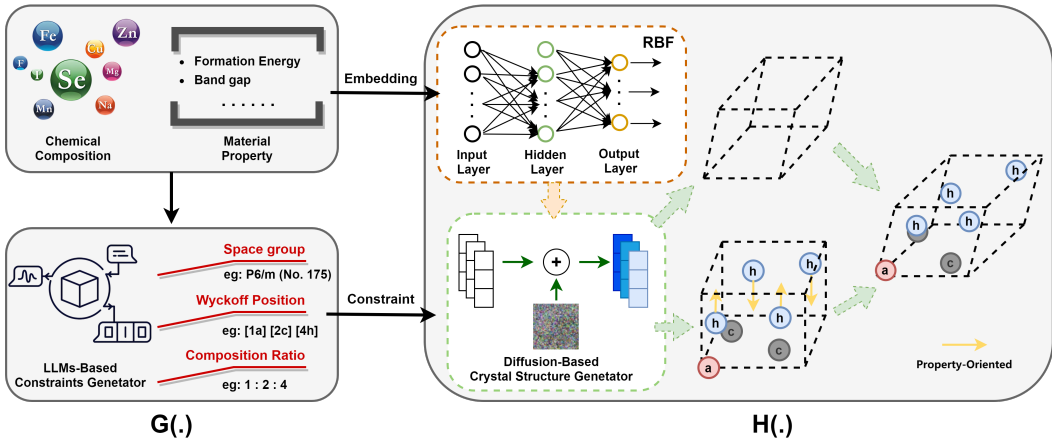


Figure 1: The schematic diagram of our proposed CrystalGF for the crystal structure generation. Where  $G(\cdot)$  denotes the constraint generation module, responsible for parsing input data and generating additional constraints;  $H(\cdot)$  represents the crystal structure generation module, which generates target crystal structures under multiple constraints.

### 3 Our method : CrystalGF

In this section, we present CrystalGF, a novel framework for crystal materials generation that synthesizes desired crystal structures guided by chemical composition and material properties.

#### 3.1 Architecture

A crystal generation model conditioned with chemical composition and material properties could be described as  $M = H(C, P)$ , where  $H(\cdot)$  represents a crystal structure generator,  $C = (c_1, c_2, \dots, c_k)$

are the chemical composition constraint in which  $k$  components are specified,  $P$  is property constraint.  $M = (A, X, L)$  represents for crystal structure, where  $A = [a_1, a_2, \dots, a_n]$  are the elemental composition of atoms inside a unit cell,  $X = [x_1, x_2, \dots, x_n] \in [0, 1)^{3 \times n}$  are fractional coordinates of  $n$  atoms,  $L = [l_1, l_2, l_3] \in \mathbb{R}^{3 \times 3}$  is the lattice. In this work, we formulate our model as:

$$M = H(G(C, P), P)$$

where  $A, S = G(C, P)$  represents a constraint generator, with  $S$  being the symmetry constraint composed of the space group type and Wyckoff positions of the target crystal structure. The framework of our two-step model is shown in Figure 1. The constraint generator  $G(\cdot)$  takes chemical composition and material properties as input and generates space group, Wyckoff positions and composition ratio, which will be taken as the input of the crystal structure generator  $H(\cdot)$  along with material properties.

Notice that for our model, the actual input constraints are still chemical composition and material properties, and we utilize a constraint generator to obtain additional constraints. We utilize a LLMs-based model as our constraint generation module (Detailed in §3.2), and a multi-conditional constrained diffusion model as the crystal structure generation module (Detailed in §3.3). Furthermore, both  $H(\cdot)$  and  $G(\cdot)$  could be any model as long as the inputs and outputs match.

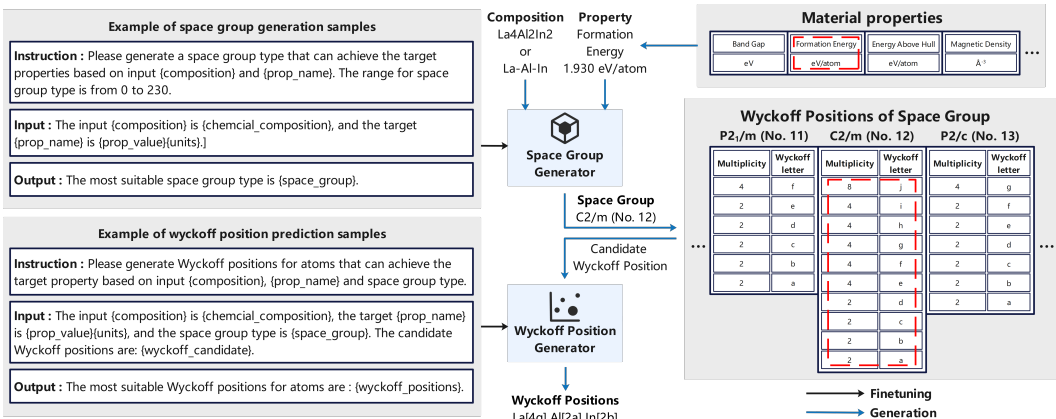


Figure 2: Overview of our constraint generator  $G(\cdot)$ . The content within curly braces represents the custom model inputs. All our prompts are in Chinese. For review purposes, only the English-translated versions are retained in the figure.

### 3.2 Constraint Generator

The constraint generator aims to generate constraints for crystal symmetry and composition ratio, where symmetry constraints include space group types and Wyckoff positions. The overall fine-tuning and inference workflow of the module is illustrated in Figure 2. Our generator is capable of receiving diverse inputs from chemical and material properties to structures, where chemical composition can be specified as either elemental composition or full chemical formulas, and material properties could include band gap, formation energy, etc. After embedding these inputs into predefined prompt templates, the module utilizes LLMs to generate corresponding symmetry constraints. Notably, when the chemical composition is provided as elemental composition, the generator simultaneously produces the corresponding composition ratio.

Since Wyckoff positions generation is related to space group types, we employ two specialized LLMs as space group generator and Wyckoff position generator, to separately generate symmetry information. First, the space group generator determines the space group of crystal unit cell based on input chemical composition and target properties. Subsequently, candidate Wyckoff letters are derived according to the space group index. Finally, the Wyckoff position generator produces corresponding Wyckoff letters for each atom based on the target properties.

We design the following three tricks in the prompts to regulate and enhance the generation results. (1) **Generation scope constraints:** For space groups, we explicitly specify in the "Instruction" part that

valid space group types should range from 0 to 230; For Wyckoff positions, we provide candidate Wyckoff letters in the "Input" part. (2) **Numerical standardization**: To minimize the impact of text length on LLMs, we standardized all input material properties by retaining three decimal places and adaptively determining appropriate units based on property types. (3) **Text optimization**: Instead of directly generating target space group type and Wyckoff positions, we incorporate the phrase "the most suitable..." into the prompts, which has been empirically shown to improve generation accuracy.

### 3.3 Crystal Structure Generator

The crystal structure generator is designed to receive symmetry constraints, elemental composition, and target properties generated by constraint generator, subsequently generating desired crystal structures. We employ a diffusion model to jointly generate the lattice matrix  $\mathbf{L}$  and fractional coordinates  $\mathbf{F}$  under these conditions. Detailed descriptions of the forward diffusion process and reverse generation procedure are provided in the B.1.

The overall architecture of our denoising model is illustrated in Figure 3, which derives two denoising terms  $\hat{\epsilon}_k, \hat{\epsilon}_{F'}$  under the constraints of elemental composition, crystal symmetry, and target properties. For feature embedding, we introduce continuous material property embeddings into input feature representations. Continuous properties, following Con-CDVAE (18), are expanded by a Gaussian Radial Basis Function (RBF) and embedded by an MLP:

$$f_{prop}(p) = \varphi_{mlp} \left( \left[ e^{-\frac{(p-p_{min})^2}{2\sigma^2}}, e^{-\frac{(p-p_{min}-\sigma)^2}{2\sigma^2}}, \dots, e^{-\frac{(p-p_{max})^2}{2\sigma^2}} \right] \right) \quad (1)$$

where  $p$  is property value,  $p_{min}$  is the preset minimum property value,  $p_{max}$  is the maximum property value, and  $\sigma$  is grid spacing of RBF. We concatenate the atom embeddings  $f_{atom}(A)$ , property embeddings  $f_{prop}(p)$  and the sinusoidal time embedding  $f_{time}(t)$  to get the input features  $C = \phi_{in}(f_{atom}(A), f_{prop}(p), f_{time}(t))$ . where  $\phi_{in}$  is a linear layer. The embedding of material properties enriches the input feature information. Compared to the strict symmetry constraints in high space groups, this approach allows the model to prioritize property-driven generation of anticipated crystal structures when operating in lower space groups with higher degrees of freedom.

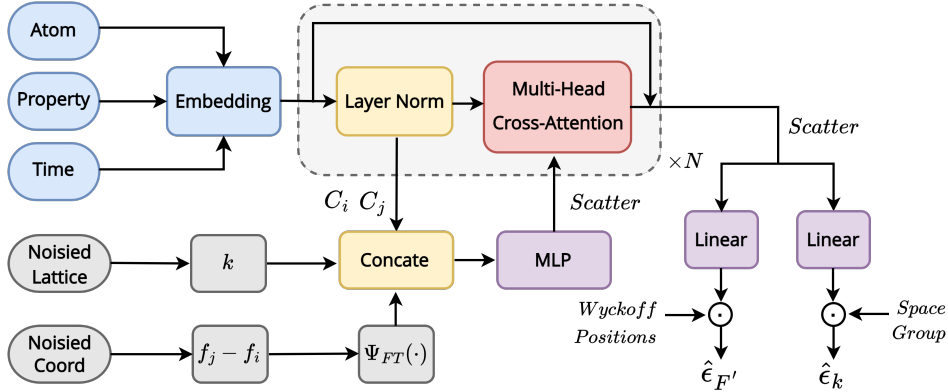


Figure 3: Diffusion model of crystal structure generator for crystal generation.

For the embedding of noisied lattices and noisied coordinates, we adopt the approach described in DiffCSP++ (16). Subsequently, we employ a multi-level cascade decoder to generate denoising terms. To enhance the model's fitting capacity, we incorporate a multi-head cross-attention mechanism within the decoder architecture to fuse information from both the noisied feature and the input feature. The structure of the decoder in the  $n$ -th layer is designed as

$$C_{ij}^{(n)} = \varphi_e \left( C_i^{(n-1)}, C_j^{(n-1)}, k, \psi_{FT}(f_j - f_i) \right), \quad (2)$$

$$C^{(n)} = C^{(n-1)} + \varphi_{mhca}(C^{(n-1)}, \sum_{j=1}^N C_{ij}^{(n)}), \quad (3)$$

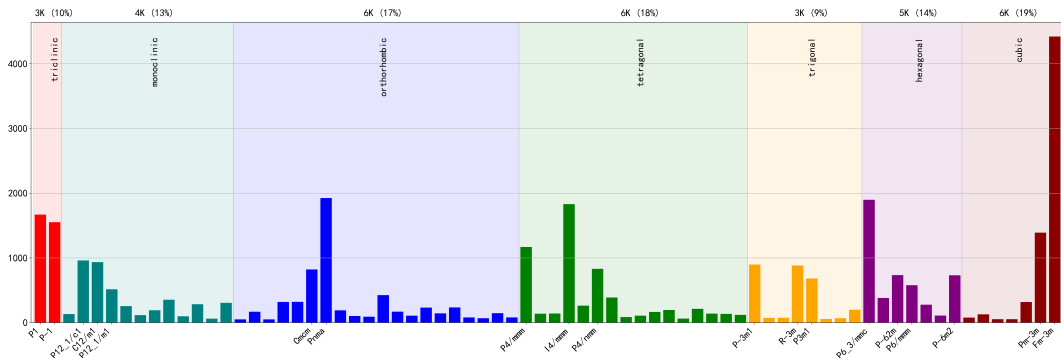


Figure 4: The distribution map of crystals across space group.

where in Eq.(2),  $C_i^{(n-1)}$  and  $C_j^{(n-1)}$  are node features extracted from  $C^{(n-1)}$ ,  $k$  is the unique  $O(3)$ -invariant representation of the lattice, and  $\psi_{FT} : (-1, 1)^3 \rightarrow [-1, 1]^{3 \times K}$  is the Fourier transformation with  $K$  bases to periodically embed the relative fractional coordinate  $f_j - f_i$ . In Eq.(3)  $\varphi_{mhca}$  is multi-head cross-attention to fuse the noised features and coordinates and the input features.

## 4 Experiments

We conducted three sets of experiments to validate the effectiveness of our framework. First, to verify the impact of the constraint generator on final crystal structure generation, we selected four different generators and demonstrated a negative correlation between symmetry accuracy and property error (Detailed in §4.1). Second, we validated the effectiveness of our multi-conditional crystal structure generator (Detailed in § 4.2). Finally, to confirm our framework’s capability to accurately generate crystal materials satisfying target property requirements, we conducted comparative experiments with MatterGen and Con-CDVAE (Detailed in §4.3).

### 4.1 Crystal Constraints Generation

We picked 34507 samples from the Materials Project (MP) (8) database, all of which were stable crystal structures, whose energy per atom after relaxation via DFT is within 0.1 eV per atom above the convex hull, with less than 20 atoms in crystal unit cell. Each sample includes a crystal structure and its associated properties, such as band gap, formation energy, energy above hull.

Input Pattern	Accuracy Rate		Space Group (%)		Wyckoff Positions (%)	
	Base LLM		Band.	Form.	Band.	Form.
Element Composition & Property	Qwen2.5-7B		32.37	30.25	59.79	59.39
	Llama-3.1-8B		<b>35.00</b>	<b>35.15</b>	<b>62.08</b>	<b>62.58</b>
	DeepSeek-R1-8B		32.22	34.28	59.38	60.92
	GLM-4-9B		33.61	32.48	60.24	60.14
Chemical Formula & Property	Qwen2.5-7B		63.66	61.66	81.43	81.94
	Llama-3.1-8B		<b>66.73</b>	<b>65.77</b>	81.10	82.02
	DeepSeek-R1-8B		65.83	65.57	81.42	80.51
	GLM-4-9B		64.76	64.36	<b>82.83</b>	<b>82.13</b>

Table 1: Accuracy rate on crystal symmetry generation.

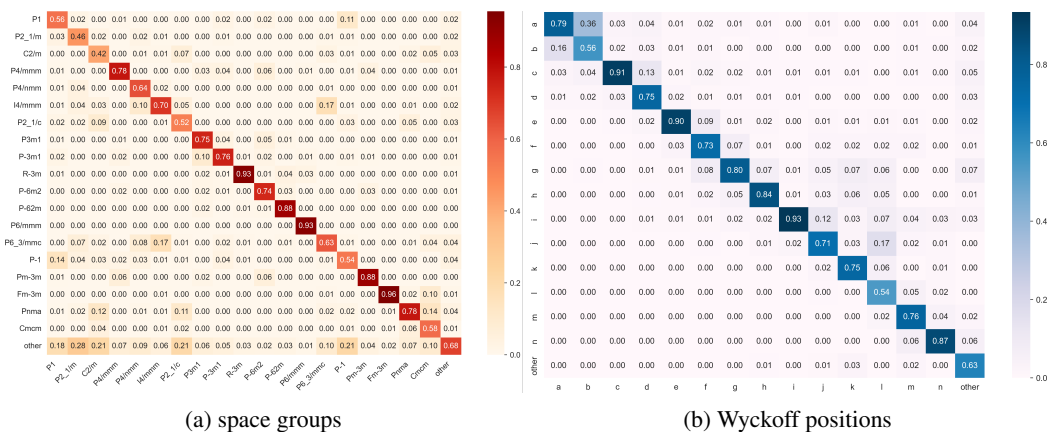


Figure 5: Confusion matrix of space groups and Wyckoff positions generation results based on chemical formula and band gap. The horizontal and vertical axis indicate true labels and predicted labels, respectively.

The distribution of crystal space group types in our dataset is visualized in Figure 4. Given the extreme sparsity for certain space group types, for instance, only 15 samples for  $I2_12_12_1$  (No.24) and 0 sample for  $Ia-3d$  (No.230), and the broad range of space group types, we adopted a strategy inspired by previous researchers (21; 22) to facilitate statistical analysis and presentation of model inference results: during model training, all original labels are preserved, but during evaluation, space group types with fewer than 500 instances are aggregated into an “other” category for statistical clarity. This approach is extended to Wyckoff positions generation, where Wyckoff letters with fewer than 50 occurrences are similarly categorized as “other”.

We selected four widely downloaded open-source LLMs under 10B as the base models for the generator and fine-tuned them using the Llama-Factory (39) framework. We provided more details in Appendix B.1. The results of the crystal symmetry generation are presented in Table 1. In experiments using elemental composition and material property as input, the highest generation accuracies for space groups and Wyckoff positions reached 35.15% and 62.58% respectively, both obtained using the Llama-based generator. When using chemical formula and material property as input, the peak accuracies for space groups and Wyckoff positions improved to 66.73% and 82.83%, achieved by the Llama-based and GLM-based generators respectively. Correspondingly, when employing four constraint generators based on different LLMs and specifying bandgap and formation energy as property constraints, the error probability distributions between the simulated properties of crystals generated by CrystalGF and target properties are presented in Tables 3 and Table 4. Combined with the results from Table 1, it demonstrates that higher symmetry accuracy achieved by constraint generators corresponds to smaller deviations between the generated crystal structures and target properties.

The confusion matrix of space groups and Wyckoff positions generation accuracy from the highest-precision constraint generator is illustrated in Figure 5. As exemplified in Figure 5a, there are five space group types that exceeded the 85% generation accuracies: 88% for  $P-62m$  (No.189), 88% for  $Pm-3m$  (No.221), 93% for  $R-3m$  (No.166), 93% for  $P6/mmm$  (No.191), and 96% for  $Fm-3m$  (No.225). These space groups correspond to crystal systems with high symmetry. On the other hand, four space groups had generation accuracies below 55%: 42% for  $C2/m$  (No.12), 46% for  $P2_1/m$  (No.11), 52% for  $P2_1/c$  (No.14), 54% for  $P-1$  (No.2). These space groups correspond to crystal systems with relatively low symmetry. We attributed this phenomenon to the fact that high-symmetry space groups (e.g., cubic crystal systems) possess greater numbers of symmetry operations and stringent geometric constraints, enabling models to more readily capture the correlations between their chemical composition and property parameters. In contrast, low-symmetry space groups (such as monoclinic or triclinic systems) exhibit complex structures with fewer symmetry elements and weaker parametric constraints. Minor variations in chemical composition or property metrics may lead to significant divergences in space group characteristics, thereby increasing the difficulty for models to learn these nonlinear relationships. In Figure 5b, the generation accuracy for Wyckoff positions of labels c, e, i, and n all exceeded 85%. In contrast, the generation accuracy for labels b

and  $l$  was relatively low but still remained around 55%. This indicates that the model can efficiently capture the symmetric atomic structure within the unit cell when given the chemical composition, target properties, and space group information.

## 4.2 Crystal Structure Generation

We evaluated our crystal structure generation module on three publicly available datasets with distinct data distributions: Perov-5, MP-20, and MPTS-52. Perov-5 (40) comprises 18,928 perovskite crystals exhibiting structural similarity but compositional diversity, each containing 5 atoms per unit cell. MP-20 (41) contains 45,231 samples representing experimentally realized crystals with  $\leq 20$  atoms per unit cell. MPTS-52 serves as a more challenging extension of MP-20, consisting of 40,476 structures with up to 52 atoms per unit cell. For all datasets, we adopt the data splitting protocols established in prior works (13; 14) to ensure benchmarking consistency. The hyper-parameters and training details are summarized in Appendix B.1.

For each generated crystal structure, we calculate the match rate through the Structure Matcher class in Pymatgen (42), with thresholds  $stol = 0.5$ ,  $angle\ tol = 10$ ,  $l\ tol = 0.3$ , following previous work. The match rate represents the ratio of matched structures relative to the total number within the testing set, and the RMSE is averaged over the matched pairs, and normalized by  $\sqrt[3]{V/N}$ , where  $V$  is the volume of the lattice,  $N$  is the atom number of crystals. We compared our approach with the following two generation-based methods, including CDVAE (13) and DiffCSP++ (16). The results of CDVAE and DiffCSP++ are obtained by reproducing the inference process using publicly released datasets and pretrained model weights.

As shown in Table 2, CrystalGF-DB and CrystalGF-DF denote models incorporating band gap and formation energy as input properties, respectively. Due to the absence of formation energy in Perov-5 dataset and band gap in MPTS-52 dataset, missing values are represented by dashes “-”. For Perov-5 dataset, our method achieves comparable performance to DiffCSP++ with matching rate of 96.27% (vs. 96.49%) and RMSE of 0.0333 (vs. 0.0343). Regarding MP-20 dataset, our approach demonstrates marginal improvements where CrystalGF-DF reaches 84.00% (vs. 83.18%) matching rate and 0.0365 (vs. 0.0351) RMSE. Notably on MPTS-52 dataset, we observe more significant enhancements with 45.38% (vs. 44.20%) matching rate and 0.0431 (vs. 0.0451) RMSE. Experimental results validate that our module achieves more pronounced improvements on complex tasks, which can be attributed to both the information fusion capability of the multi-head cross-attention mechanism and the property-oriented generation capacity of module in low symmetry environments enabled by property embedding optimization. In addition, the band gap based model exhibits certain performance degradation in Perov-5 dataset, which we speculated stems from the excessive sparsity of input feature representations caused by numerous band gap values approaching zero, leading to suboptimal results.

	Perov-5		MP-20		MPTS-52	
	MR(%)	RMSE	MR(%)	RMSE	MR(%)	RMSE
CDVAE	48.58	0.1009	35.66	0.1020	6.16	0.1904
DiffCSP++	<b>96.49</b>	0.0343	83.18	0.0351	44.20	0.0451
CrystalGF-DB	96.27	<b>0.0333</b>	83.20	<b>0.0345</b>	-	-
CrystalGF-DF	-	-	<b>84.00</b>	0.0365	<b>45.38</b>	<b>0.0431</b>

Table 2: Results on crystal structure generation. MR stands for Match Rate.

## 4.3 Material Properties Comparison

In this subsection, we compared the differences between the simulated properties of the generated structures and the target properties. We employ density functional theory (DFT) for computational simulations using the Vienna Ab initio Simulation Package (43) (44) (VASP), more details in Appendix B.3. For comparative analysis, we fine-tuned and retrained two multi-conditional crystal generation models: MatterGen and Con-CDVAE, the training details are provided in the appendix B.1. In practical crystal materials design, it is considered acceptable if the absolute error of the properties is less than 0.05, and meet the requirement if less than 0.01, and the unit of band gap and formation

energy are eV and eV/atom, respectively. Therefore, we compared the probability distributions of property absolute errors between different models in Tables 3 and Table 4.

Our framework benefits from the precise symmetry and composition ratio generation of the constraint generator, along with the strict multi-conditional constraints imposed by the structure generator, enabling higher precision of generating crystal structures with target inputs.

In generation tasks targeting elemental composition and material properties, our method demonstrates improvements over MatterGen in both property and composition constraint capabilities. Specifically, CrystalGF, when using LLaMA as the base constraint-aware generator, achieves a 10% improvement in elemental precision compared to MatterGen. Moreover, structures generated by our approach are more than twice as likely to satisfy the target properties relative to prior generative models. In particular, CrystalGF doubles the success rate of MatterGen in generating structures with formation energy differences below 0.01 eV/atom.

For generation tasks targeting chemical formulas and material properties, Specifically, it achieves nearly 100% compliance with elemental constraints, whereas Con-CDVAE attains an average probability of only 5.81%. This disparity is primarily attributed to Con-CDVAE’s limitation of modeling only structural and property distributions during its initial training phase. In terms of property constraints, CrystalGF, when using GLM as the constraint-aware generative base model, achieves approximately 30% higher probability than Con-CDVAE in generating structures with formation energy differences below 0.05 eV/atom.

We present partially generation results exhibiting high similarity to structures in the test set in Figures 7. Owing to precise symmetry constraint generation and the superior accuracy of our structure generator trained on the MP dataset, the generated structures closely resemble their MP counterparts, resulting in nearly identical computational material properties. Meanwhile, Figure 8 showcases generated structures that deviate more noticeably from the test set. Although these structures exhibit partial discrepancies in symmetry constraint generations compared to original data, their computed properties remain proximate to target values. Notably, no analogous structures exist in the MP dataset, highlighting the capability of our framework not only to accurately reproduce known materials but also to discover novel ones.

## 5 Conclusion

In this work, we propose CrystalGF, a generation framework with strict constraints for crystal generation. We decompose the generation process into intermediate constraint generation and structural generation. Within our framework, intermediate constraints such as symmetry and component ratios are generated by a LLMs-based constraint generator according to chemical composition and target properties, which are strictly enforced by a diffusion-based crystal generator to ensure constraint-controlled structure generation. Experimental results demonstrate that compared with previous methods, structures produced by our method are more than twice as likely to meeting the target properties, while maintaining rigorous adherence to input chemical composition. We believe that the multiple strict constraint ability of our method represent an important advance towards automatically and accurately designing of crystal materials. Furthermore, it could be extended in many directions, such as covering more physical and chemical properties or transferring to other research areas like molecules generation.

Method	Error Bars	Prob. of BG (%)		Comp.(%)	Prob. of FE (%)		Comp.(%)
		< 0.01	< 0.05		< 0.01	< 0.05	
MatterGen		48.69	63.03	89.80	3.30	15.90	84.28
CrystalGF (Qwen)		48.29	<b>66.49</b>	<b>100.00</b>	5.73	20.85	99.96
CrystalGF (DS)		48.96	65.92	99.98	6.41	23.67	99.96
CrystalGF (GLM)		48.07	66.27	99.98	6.37	22.86	99.97
CrystalGF (Llama)		<b>48.87</b>	66.38	99.97	<b>6.81</b>	<b>24.68</b>	<b>99.98</b>

Table 3: The probability distribution of property absolute errors and precision of chemical composition of crystal structures generated by elemental composition and material properties.

Method	Error Bars	Prob. of BG (%)		Comp.(%)	Prob. of FE (%)		Comp.(%)
		< 0.01	< 0.05		< 0.01	< 0.05	
Con-CDVAE		<b>56.13</b>	64.33	7.02	0.63	2.92	4.33
CrystalGF (Qwen)		49.78	67.61	<b>100.00</b>	11.28	32.68	99.99
CrystalGF (Llama)		49.64	67.64	<b>100.00</b>	11.71	<b>33.90</b>	99.98
CrystalGF (DS)		49.82	67.88	<b>100.00</b>	11.43	32.59	99.99
CrystalGF (GLM)		49.47	<b>67.96</b>	<b>100.00</b>	<b>12.02</b>	33.74	<b>100.00</b>

Table 4: The probability distribution of property absolute errors and precision of chemical composition of crystal structures generated by chemical formula and material properties.

## References

- [1] Maylis Orio, Dimitrios A Pantazis, and Frank Neese. Density functional theory. *Photosynthesis research*, 102:443–453, 2009.
- [2] Zhenpeng Yao, Yanwei Lum, Andrew Johnston, Luis Martin Mejia-Mendoza, Xin Zhou, Yonggang Wen, Alán Aspuru-Guzik, Edward H Sargent, and Zhi Wei Seh. Machine learning for a sustainable energy future. *Nature Reviews Materials*, 8(3):202–215, 2023.
- [3] Jake Graser, Steven K Kauwe, and Taylor D Sparks. Machine learning and energy minimization approaches for crystal structure predictions: a review and new horizons. *Chemistry of Materials*, 30(11):3601–3612, 2018.
- [4] Jakob Timmermann, Florian Kraushofer, Nikolaus Resch, Peigang Li, Yu Wang, Zhiqiang Mao, Michele Riva, Yonghyuk Lee, Carsten Staacke, Michael Schmid, et al. Iro 2 surface complexions identified through machine learning and surface investigations. *Physical review letters*, 125(20):206101, 2020.
- [5] Shiyue Yang and Graeme M Day. Exploration and optimization in crystal structure prediction: Combining basin hopping with quasi-random sampling. *Journal of Chemical Theory and Computation*, 17(3):1988–1999, 2021.
- [6] Gowoon Cheon, Lusann Yang, Kevin McCloskey, Evan J Reed, and Ekin D Cubuk. Crystal structure search with random relaxations using graph networks. *arXiv preprint arXiv:2012.02920*, 6, 2020.
- [7] Jinyu Liu. Cspth: A crystal structure prediction framework on tianhe-2 supercomputer. *Computer Science and Application*, 2022.
- [8] Anubhav Jain, Shyue Ping Ong, Geoffroy Hautier, Wei Chen, William Davidson Richards, Stephen Dacek, Shreyas Cholia, Dan Gunter, David Skinner, Gerbrand Ceder, et al. Commentary: The materials project: A materials genome approach to accelerating materials innovation. *APL materials*, 1(1), 2013.
- [9] Jonathan Schmidt, Noah Hoffmann, Hai-Chen Wang, Pedro Borlido, Pedro JMA Carriço, Tiago FT Cerqueira, Silvana Botti, and Miguel AL Marques. Large-scale machine-learning-assisted exploration of the whole materials space. *arXiv preprint arXiv:2210.00579*, 2022.
- [10] Jonathan Schmidt, Hai-Chen Wang, Tiago FT Cerqueira, Silvana Botti, and Miguel AL Marques. A dataset of 175k stable and metastable materials calculated with the pbesol and scan functionals. *Scientific Data*, 9(1):64, 2022.
- [11] Asma Noura, Nataliya Sokolovska, and Jean-Claude Crivello. Crystalgan: learning to discover crystallographic structures with generative adversarial networks. *arXiv preprint arXiv:1810.11203*, 2018.
- [12] Zekun Ren, Siyu Isaac Parker Tian, Juhwan Noh, Felipe Oviedo, Guangzong Xing, Jiali Li, Qiaohao Liang, Ruiming Zhu, Armin G Aberle, Shijing Sun, et al. An invertible crystallographic representation for general inverse design of inorganic crystals with targeted properties. *Matter*, 5(1):314–335, 2022.
- [13] Tian Xie, Xiang Fu, Octavian-Eugen Ganea, Regina Barzilay, and Tommi Jaakkola. Crystal diffusion variational autoencoder for periodic material generation. *arXiv preprint arXiv:2110.06197*, 2021.
- [14] Rui Jiao, Wenbing Huang, Peijia Lin, Jiaqi Han, Pin Chen, Yutong Lu, and Yang Liu. Crystal structure prediction by joint equivariant diffusion. *Advances in Neural Information Processing Systems*, 36, 2024.
- [15] Zhendong Cao, Xiaoshan Luo, Jian Lv, and Lei Wang. Space group informed transformer for crystalline materials generation. *arXiv preprint arXiv:2403.15734*, 2024.

- [16] Rui Jiao, Wenbing Huang, Yu Liu, Deli Zhao, and Yang Liu. Space group constrained crystal generation. *arXiv preprint arXiv:2402.03992*, 2024.
- [17] Claudio Zeni, Robert Pinsler, Daniel Zügner, Andrew Fowler, Matthew Horton, Xiang Fu, Sasha Shysheya, Jonathan Crabbé, Lixin Sun, Jake Smith, et al. Mattergen: a generative model for inorganic materials design. *arXiv preprint arXiv:2312.03687*, 2023.
- [18] Cai-Yuan Ye, Hong-Ming Weng, and Quan-Sheng Wu. Con-cdvae: A method for the conditional generation of crystal structures. *Computational Materials Today*, 1:100003, 2024.
- [19] Sherry Yang, KwangHwan Cho, Amil Merchant, Pieter Abbeel, Dale Schuurmans, Igor Mordatch, and Ekin Dogus Cubuk. Scalable diffusion for materials generation. *arXiv preprint arXiv:2311.09235*, 2023.
- [20] Yong Zhao, Yuxin Cui, Zheng Xiong, Jing Jin, Zhonghao Liu, Rongzhi Dong, and Jianjun Hu. Machine learning-based prediction of crystal systems and space groups from inorganic materials compositions. *ACS omega*, 5(7):3596–3606, 2020.
- [21] Y Che, D Wang, H Lv, and X Wu. Crystal system and space group prediction of two-dimensional materials from chemical formula via deep neural networks. *Materials Today Chemistry*, 33:101667, 2023.
- [22] Da-yong Wang, Hai-feng Lv, and Xiao-jun Wu. Crystallographic groups prediction from chemical composition via deep learning. *Chinese Journal of Chemical Physics*, 36(1):66–74, 2023.
- [23] Minglei Bai, Haoxuan Diao, Xijiao Mu, Zhong Wang, Jing Cao, and Yuee Li. Rewc-gnn algorithm for the property prediction of large-scale crystals. *The Journal of Physical Chemistry A*, 128(30):6183–6189, 2024.
- [24] Gemini Team, Petko Georgiev, Ving Ian Lei, Ryan Burnell, Libin Bai, Anmol Gulati, Garrett Tanzer, Damien Vincent, Zhufeng Pan, Shibo Wang, et al. Gemini 1.5: Unlocking multimodal understanding across millions of tokens of context. *arXiv preprint arXiv:2403.05530*, 2024.
- [25] Aaron Hurst, Adam Lerer, Adam P Goucher, Adam Perelman, Aditya Ramesh, Aidan Clark, AJ Ostrow, Akila Welihinda, Alan Hayes, Alec Radford, et al. Gpt-4o system card. *arXiv preprint arXiv:2410.21276*, 2024.
- [26] Aixin Liu, Bei Feng, Bing Xue, Bingxuan Wang, Bochao Wu, Chengda Lu, Chenggang Zhao, Chengqi Deng, Chenyu Zhang, Chong Ruan, et al. Deepseek-v3 technical report. *arXiv preprint arXiv:2412.19437*, 2024.
- [27] Daya Guo, Dejian Yang, Haowei Zhang, Junxiao Song, Ruoyu Zhang, Runxin Xu, Qihao Zhu, Shirong Ma, Peiyi Wang, Xiao Bi, et al. Deepseek-r1: Incentivizing reasoning capability in llms via reinforcement learning. *arXiv preprint arXiv:2501.12948*, 2025.
- [28] Hugo Touvron, Thibaut Lavril, Gautier Izacard, Xavier Martinet, Marie-Anne Lachaux, Timothée Lacroix, Baptiste Rozière, Naman Goyal, Eric Hambro, Faisal Azhar, et al. Llama: Open and efficient foundation language models. *arXiv preprint arXiv:2302.13971*, 2023.
- [29] Aaron Grattafiori, Abhimanyu Dubey, Abhinav Jauhri, Abhinav Pandey, Abhishek Kadian, Ahmad Al-Dahle, Aiesha Letman, Akhil Mathur, Alan Schelten, Alex Vaughan, et al. The llama 3 herd of models. *arXiv preprint arXiv:2407.21783*, 2024.
- [30] Jinze Bai, Shuai Bai, Yunfei Chu, Zeyu Cui, Kai Dang, Xiaodong Deng, Yang Fan, Wenbin Ge, Yu Han, Fei Huang, et al. Qwen technical report. *arXiv preprint arXiv:2309.16609*, 2023.
- [31] An Yang, Baosong Yang, Beichen Zhang, Binyuan Hui, Bo Zheng, Bowen Yu, Chengyuan Li, Dayiheng Liu, Fei Huang, Haoran Wei, et al. Qwen2. 5 technical report. *arXiv preprint arXiv:2412.15115*, 2024.
- [32] Zhengxiao Du, Yujie Qian, Xiao Liu, Ming Ding, Jiezhong Qiu, Zhilin Yang, and Jie Tang. Glm: General language model pretraining with autoregressive blank infilling. *arXiv preprint arXiv:2103.10360*, 2021.
- [33] Team GLM, Aohan Zeng, Bin Xu, Bowen Wang, Chenhui Zhang, Da Yin, Dan Zhang, Diego Rojas, Guanyu Feng, Hanlin Zhao, et al. Chatglm: A family of large language models from glm-130b to glm-4 all tools. *arXiv preprint arXiv:2406.12793*, 2024.
- [34] Zi-Yi Chen, Fan-Kai Xie, Meng Wan, Yang Yuan, Miao Liu, Zong-Guo Wang, Sheng Meng, and Yan-Gang Wang. Matchat: A large language model and application service platform for materials science. *Chinese Physics B*, 32(11):118104, 2023.

- [35] Yingheng Tang, Wenbin Xu, Jie Cao, Jianzhu Ma, Weilu Gao, Steve Farrell, Benjamin Erichson, Michael W Mahoney, Andy Nonaka, and Zhi Yao. Matterchat: A multi-modal llm for material science. *arXiv preprint arXiv:2502.13107*, 2025.
- [36] Shuyi Jia, Chao Zhang, and Victor Fung. Lmatdesign: Autonomous materials discovery with large language models. *arXiv preprint arXiv:2406.13163*, 2024.
- [37] Fankai Xie, Tenglong Lu, Sheng Meng, and Miao Liu. Gptff: A high-accuracy out-of-the-box universal ai force field for arbitrary inorganic materials. *Science Bulletin*, 69(22):3525–3532, 2024.
- [38] Luis M Antunes, Keith T Butler, and Ricardo Grau-Crespo. Crystal structure generation with autoregressive large language modeling. *Nature Communications*, 15(1):1–16, 2024.
- [39] Yaowei Zheng, Richong Zhang, Junhao Zhang, Yanhan Ye, Zheyang Luo, Zhangchi Feng, and Yongqiang Ma. Llamafactory: Unified efficient fine-tuning of 100+ language models. *arXiv preprint arXiv:2403.13372*, 2024.
- [40] Ivano E Castelli, David D Landis, Kristian S Thygesen, Søren Dahl, Ib Chorkendorff, Thomas F Jaramillo, and Karsten W Jacobsen. New cubic perovskites for one-and two-photon water splitting using the computational materials repository. *Energy & Environmental Science*, 5(10):9034–9043, 2012.
- [41] A Jain, SP Ong, G Hautier, W Chen, WD Richards, S Dacek, S Cholia, D Gunter, D Skinner, G Ceder, et al. The materials project: a materials genome approach to accelerating materials innovation. *apl mater* 1: 011002, 2013.
- [42] Shyue Ping Ong, William Davidson Richards, Anubhav Jain, Geoffroy Hautier, Michael Kocher, Shreyas Cholia, Dan Gunter, Vincent L Chevrier, Kristin A Persson, and Gerbrand Ceder. Python materials genomics (pymatgen): A robust, open-source python library for materials analysis. *Computational Materials Science*, 68:314–319, 2013.
- [43] Georg Kresse and Jürgen Furthmüller. Efficient iterative schemes for ab initio total-energy calculations using a plane-wave basis set. *Physical review B*, 54(16):11169, 1996.
- [44] Georg Kresse and Jürgen Furthmüller. Efficiency of ab-initio total energy calculations for metals and semiconductors using a plane-wave basis set. *Computational materials science*, 6(1):15–50, 1996.
- [45] Ashish Vaswani, Noam Shazeer, Niki Parmar, Jakob Uszkoreit, Llion Jones, Aidan N Gomez, Łukasz Kaiser, and Illia Polosukhin. Attention is all you need. *Advances in neural information processing systems*, 30, 2017.

## A Crystal Supplementary Know

### A.1 Crystal Structure representation

Any crystal structure  $M$  can be described as the periodic arrangement of atoms in 3D space. The repeating unit is called a unit cell. A unit cell that includes  $n$  atoms can be fully described by a triplet, denoted as  $(A, X, L)$ , where  $A = [a_1, a_2, \dots, a_n] \in \mathbb{R}^{h \times n}$  represents the one-hot representations of atom type,  $X = [x_1, x_2, \dots, x_n] \in \mathbb{R}^{3 \times n}$  comprises the coordinates of atoms, and  $L = [l_1, l_2, l_3] \in \mathbb{R}^{3 \times 3}$  is the lattice matrix containing three basic vectors to periodically translate the unit cell to the entire 3D space. The infinite periodic structure  $M = (A, X, L)$  can be represented as

$$M := \left\{ \left( a_i, x_i' \right) \mid x_i' = x_i + \sum_{i=1}^3 k_i l_i, k_i \in \mathbb{Z} \right\} \quad (4)$$

where  $k_i$  are any integers that translate the unit cell using  $L$  to tile the entire 3D space.

### A.2 Crystal Symmetry Constraint

Crystal symmetry, encompassing space groups and Wyckoff positions, plays a pivotal role in the description of crystal structures. We illustrate the influence of space group types on lattice parameters in Table 5. Space group types are numbered from 0 to 230 and correspond to the seven crystal systems. Among them, Space groups with higher numerical indices impose more stringent lattice constraints. For instance, 195 ~ 230 belong to the cubic system, where the lattice adopts a cube-shaped configuration with only one degree of freedom in lattice parameters. Conversely, 1 ~ 2 correspond to the triclinic system, featuring lattices of arbitrary geometry with six degrees of freedom. The trigonal system presents a unique case, incorporating both rhombohedral and hexagonal lattice configurations, thereby encompassing two distinct types of lattice constraints.

Table 5: The constraint of space group types on lattice shape, where a, b, c represent the lengths of the lattice vectors, and  $\alpha, \beta, \gamma$  represent the angles between them.

Crystal System	Space Group	Length Constraint	Angle Constraint
Triclinic	1 ~ 2	$a \neq b \neq c$	$\alpha \neq \beta \neq \gamma$
Monoclinic	3 ~ 15	$a \neq b \neq c$	$\alpha = \gamma = 90^\circ, \beta \neq 90^\circ$
Orthorhombic	16 ~ 74	$a \neq b \neq c$	$\alpha = \beta = \gamma = 90^\circ$
Tetragonal	75 ~ 142	$a = b \neq c$	$\alpha = \beta = \gamma = 90^\circ$
Trigonal	143 ~ 167	$a = b = c$	$\alpha = \beta = \gamma \neq 90^\circ$
		$a = b \neq c$	$\alpha = \beta = 90^\circ, \gamma = 120^\circ$
Hexagonal	168 ~ 194	$a = b \neq c$	$\alpha = \beta = 90^\circ, \gamma = 120^\circ$
Cubic	195 ~ 230	$a = b = c$	$\alpha = \beta = \gamma = 90^\circ$

We present a three-dimensional schematic in Figure 6 to demonstrate the constraints of Wyckoff positions in space group  $P2_1/m$  (No. 11) on atomic fractional coordinates. Rhombuses denote Wyckoff letters with fixed coordinates. Due to the periodicity of the unit cell, corner atoms exhibit 1/8 occupancy, edge atoms 1/4 occupancy, and face-centered atoms 1/2 occupancy. Taking Wyckoff letter 'a' as an example, its multiplicity of 2 arises from eight corner-located atoms and four edge-located atoms. Circular and elliptical symbols represent Wyckoff positions with variable coordinates: atoms in circular sites (orange) are constrained by mirror planes with two degrees of freedom, while elliptical sites allow three degrees of freedom governed by interatomic positional relationships.

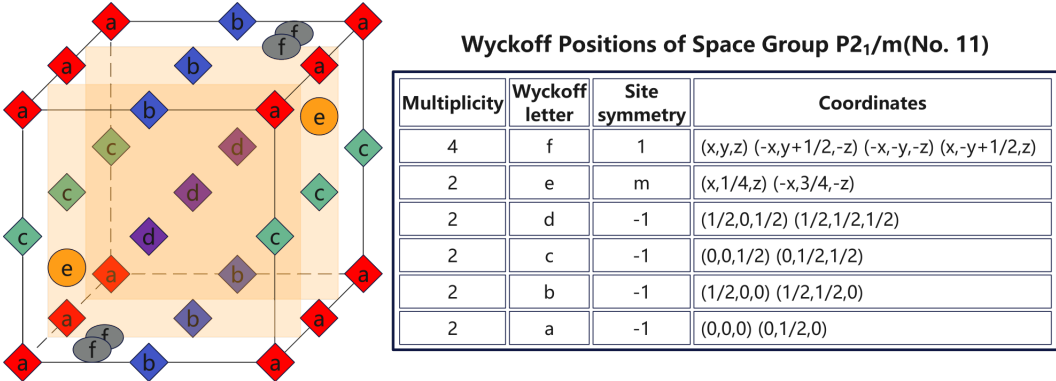


Figure 6: The Impact of Wyckoff Positions of Group  $P2_1/m$  (No. 11) on Atomic Coordinates.

## B Implementation Details

### B.1 Hyper-parameters and Training Details

We train CDVAE (13), DiffCSP++ (16), and our crystal structure generator on three public datasets to validate the effectiveness of the structure generator. Using the dataset described in Section §4.1, we train Con-CDVAE (18), MatterGen (17), and our CrystalGF to verify the validity of the overall framework. We split our data into 80% training, 10% validation, and 10% test sets while maintaining strict correspondence between space group and Wyckoff positions entries, this operation prevents data leakage by ensuring identical crystals are allocated to the same subset. To the best of our knowledge, Con-CDVAE and MatterGen represent the advanced multi-conditional generative models, which utilize chemical formulas with material properties and elemental composition with material properties as model inputs, respectively. Therefore, we conduct comparative evaluations of both models against our CrystalGF.

For CDVAE, we apply the transformer-enhanced (45) version of CDVAE as introduced in DiffCSP (14), while maintaining consistent training parameters. For DiffCSP++, we train the denoising model with 6 layers, 512-dimension hidden layer, and 128-dimension Fourier embeddings and the training epochs are set to 3000, 1500, 1000 for Perov-5, MP-20, and MPTS-52. For MatterGen, we fine-tuning the pre-trained model with chemical system and property, including band gap and formation energy. The dimension of the property embedding and the chemical system multi-hot embedding is set to 512, and model is trained for 1000 epochs with an Adam optimizer with initial learning rate  $5 \times 10^{-6}$  and a Plateau scheduler with a decaying factor 0.6 and a patience of 100 epochs. For Con-CDVAE, we train model with chemical formula and property, including band gap and formation energy. The formula embedding module has 3 layers, 92-dimension input layer and 64-dimension hidden layer, the property embedding module has 3 layers and 64-dimension hidden layer and the model is trained for 1000 epochs with an Adam optimizer with initial learning rate  $1 \times 10^{-3}$  and a Plateau scheduler with a decaying factor 0.6 and a patience of 30 epochs.

For our symmetry generator, We fine-tune four LLMs ,including Qwen2.5-7B-Instruct, Llama-3.1-8B-Instruct, DeepSeek-R1-8B, and GLM-4-9B-chat, using LoRA from Llamafactory (39) framework. The LoRA fine-tuning specifically targets the qkv layers in transformer modules with 20 epochs and a  $1 \times 10^{-4}$  initial learning rate, the learning rate scheduler type is set to cosine annealing strategy with 0.1 warm up ratio. And the fine-tuning precision is set to FP32 throughout all computations.

For our Structure generator, we apply the input features consist of 512-dimension atom embeddings, 128-dimension property embeddings and 128-dimension Fourier embeddings. The decoder employs 6 layers with 512 hidden states and multi-head cross-attention using num\_heads = 2. The training epochs are configured as 3000 for Perov-5, 1500 for MP-20, and 1000 for MPTS-52. Optimization utilizes Adam with an initial learning rate of  $1 \times 10^{-3}$ , coupled with a ReduceLRonPlateau scheduler that reduces the learning rate by 0.6 factor and 30 patience. All models are trained on A40 GPU.

Table 6: The constraint of space group types on lattice shape, where a, b, c represent the lengths of the lattice vectors, and  $\alpha, \beta, \gamma$  represent the angles between them.

Model Training	Computer Work	Memory Usage	Time Usage
CDVAE		12GB	10h
Con-CDVAE		24GB	12h
DiffCSP++	NVIDIA A40 GPU	24GB	30h
MatterGen		45GB	50h
Constraint Generator		26GB + 30GB	9h + 18h
Structure Generator		30GB	46h

## B.2 Symmetry Accuracy Details

For the evaluation of space group generation accuracy, we directly compare the outputs with the labels from the dataset. Regarding Wyckoff position generation accuracy, since different Wyckoff letters correspond to varying multiplicities across space groups, we exclusively calculate the accuracy of Wyckoff letters. Notably, a type of atom may possess multiple Wyckoff letters, and the generation order of these letters should not affect accuracy statistics. For instance, the sequences Ba[4d] Ba[6g] and Ba[6g] Ba[4d] should be considered equivalent.

When constructing the confusion matrix for Wyckoff positions generation, we first identify matches where both the atomic order and generated letters coincide. Second, we distinguish cases where generated letters match despite atomic order discrepancies. Finally, atoms with inconsistent generation quantities are handled by padding with an "other" category.

## B.3 DFT Calculation Details

We employ density functional theory (DFT) for computational simulations using the VASP (43) (44), which implements the projector augmented wave (PAW) method, to conduct material property simulations and validation calculations. The generalized gradient approximation (GGA) with the Perdew-Burke-Ernzerhof (PBE) functional was adopted to treat exchange-correlation interactions. In our simulations, we set a plane-wave energy cutoff of 500 eV for the basis set and utilized a Gamma-centered k-point mesh with a grid spacing of  $0.06\pi \text{ \AA}^{-1}$ . The total energy convergence criterion was set to  $1.0 \times 10^{-1}$  eV. Post-processing of data obtained from VASP was performed using the VASPKIT toolkit.

We calculate band gap and formation energy of generated materials. The band gap is defined as the energy interval between the valence band maximum (VBM) and the conduction band minimum (CBM). Using VASP, we performed two-step calculations: self-consistent field (SCF) and non-self-consistent field (NSCF) computations, followed by post-processing with vaspkit to obtain simulation-validated bandgap values, which were compared with generated band gap results.

The formation energy refers to the energy released when a compound is synthesized from its constituent elemental phases. For a binary compound  $A_m B_n$ , its formation energy can be expressed as:

$$E_f = \frac{E(A_m B_n) - m \times E(A) - n \times E(B)}{m + n} \quad (5)$$

where  $E(A_m B_n)$  represents the total energy of the compound  $A_m B_n$ , while  $E(A)$  and  $E(B)$  denote the normalized energies of the corresponding elements A and B, respectively.

By using a batch processing method, we calculated the total energy of the compound and the corresponding elements using the VASP software package, and obtained the formation energy based on the Eq.(5).

## B.4 Experiments Compute Resources

We present the computational resources consumed for training in Table 6, including GPU type, memory usage, and training duration. The resource consumption for CDVAE and DiffCSP++ corresponds to training with the MP-20 dataset mentioned in §4.2, while Con-CDVAE, MatterGen, the Constraint Generator, and the Structure Generator reflect the resource usage when trained on the dataset described in §4.1.

In the DFT calculations, we perform VASP simulations on the generated crystal structures using the Hygon 7380 CPU. The formation energy calculations required 1.92 core-hours per structure, while the band gap calculations consumed 3.84 core-hours per structure and we consume approximately 100000 core-hours in total.

## C Visualization of Generated Crystals Structures

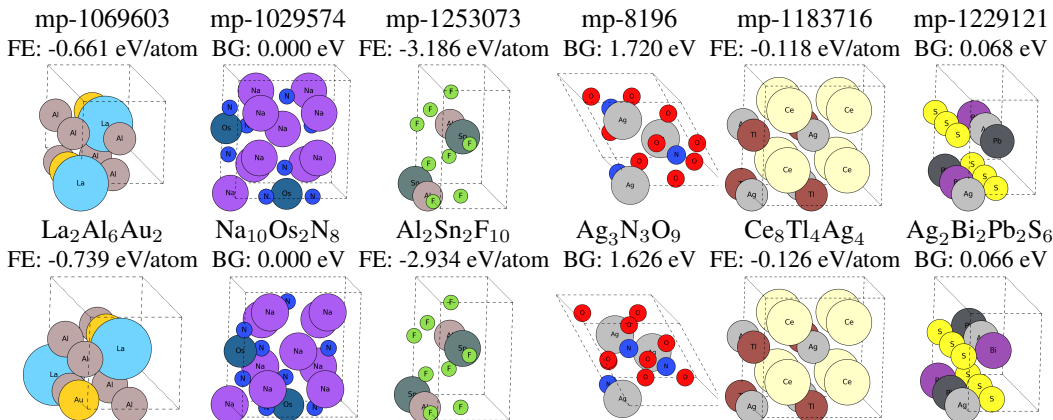


Figure 7: Crystal structures generated by CrystalGF exhibit the same symmetry and similar material properties as those in the MP database.

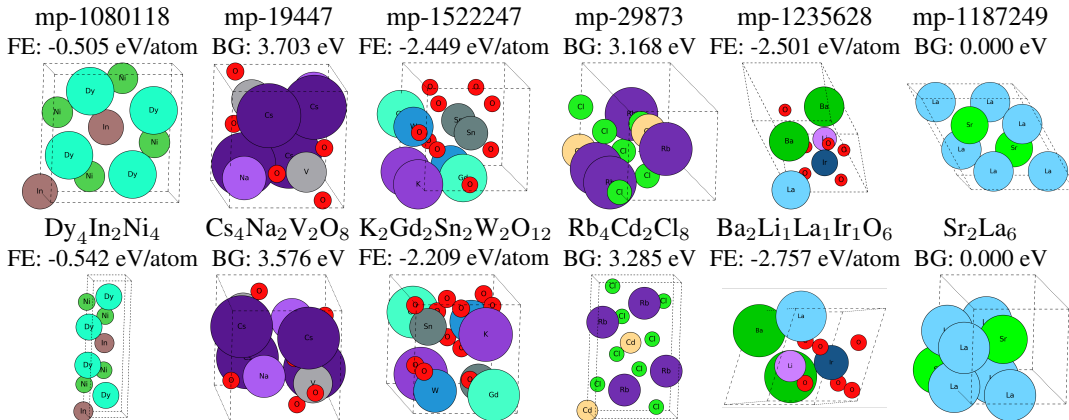


Figure 8: Crystal structures generated by CrystalGF exhibit the different symmetry but similar material properties as those in the MP dataset.

## D Societal Impacts

Our proposed strictly constrained crystal structure generation framework represents a data-driven methodology that constitutes both a significant technological progress in materials science and a development with complex societal implications.

Traditional research and development of crystal materials are based on experimental trial and error, often over decades. Our structure generation framework addresses this challenge by analyzing extensive known structural data to generate target crystals within a broader symmetry space, thereby compressing material development cycles to weeks or even days while significantly reducing human resources, material costs, and time investment.

However, critical challenges remain. Sensitive data involved in advanced material development (e.g., military-grade material formulations) require the establishment of trusted data management platforms with robust data-sharing protocols and incentive mechanisms. Furthermore, data-driven crystal generation methods present emerging concerns including ambiguous copyright ownership and potential model hallucinations. These generated results should be cross-validated through rigorous experiments and expert review rather than being blindly relied upon.

## **E Limitations**

We employ LLMs as the base models for our constraints generator, which significantly enhances the ability of our framework to learn complex relationships between material properties, chemical composition, and symmetry. However, this architecture increases computational costs for both fine-tuning and practical deployment. And through tens of thousands generation tests, we observe that in formula and property guided generation, approximately 0.069% of cases exhibited failure in subsequent Wyckoff positions generation due to erroneous space group generation.

Furthermore, it can be found in Table 1 that while different generators show comparable overall performance within the same task, symmetry generation accuracy based on elemental composition showed significant inferiority compared to formula-based approaches. We attribute this discrepancy to the inherent structural information embedded in chemical formulas: Standard chemical formulas (e.g.,  $\text{Fe}_2\text{O}_3$  or  $\text{TiO}_2$ ) not only specify elemental composition but also implicitly encode potential bonding configurations and structural tendencies (e.g., spinel or rutile configurations), thereby providing more definitive classification clues. In contrast, mere elemental composition (e.g., Fe-O or Ti-O) lack constraints on atomic quantities and bonding patterns, forcing models to deduce complex symmetries from ambiguous inputs. Furthermore, the strong correlations between standard chemical formulas and space group classifications in existing material databases enable formula-based models to better capture structural patterns from training data. Conversely, models relying solely on elemental composition must contend with higher-dimensional uncertainties, as identical elemental composition may correspond to multiple compounds with distinct space groups, consequently diminishing generation accuracy.

## NeurIPS Paper Checklist

### 1. Claims

Question: Do the main claims made in the abstract and introduction accurately reflect the paper's contributions and scope?

Answer: [Yes]

Justification: In the abstract and the latter part of the introduction, we explicitly state the scope of this work as crystal structure generation. The principal contribution of this paper lies in proposing a two-stage strict constrained generation framework, which demonstrates a 16% reduction in RMSE for generating crystals with target property compared to state-of-the-art approaches.

Guidelines:

- The answer NA means that the abstract and introduction do not include the claims made in the paper.
- The abstract and/or introduction should clearly state the claims made, including the contributions made in the paper and important assumptions and limitations. A No or NA answer to this question will not be perceived well by the reviewers.
- The claims made should match theoretical and experimental results, and reflect how much the results can be expected to generalize to other settings.
- It is fine to include aspirational goals as motivation as long as it is clear that these goals are not attained by the paper.

### 2. Limitations

Question: Does the paper discuss the limitations of the work performed by the authors?

Answer: [Yes]

Justification: We discuss the limitations of the proposed method in Appendix E.

Guidelines:

- The answer NA means that the paper has no limitation while the answer No means that the paper has limitations, but those are not discussed in the paper.
- The authors are encouraged to create a separate "Limitations" section in their paper.
- The paper should point out any strong assumptions and how robust the results are to violations of these assumptions (e.g., independence assumptions, noiseless settings, model well-specification, asymptotic approximations only holding locally). The authors should reflect on how these assumptions might be violated in practice and what the implications would be.
- The authors should reflect on the scope of the claims made, e.g., if the approach was only tested on a few datasets or with a few runs. In general, empirical results often depend on implicit assumptions, which should be articulated.
- The authors should reflect on the factors that influence the performance of the approach. For example, a facial recognition algorithm may perform poorly when image resolution is low or images are taken in low lighting. Or a speech-to-text system might not be used reliably to provide closed captions for online lectures because it fails to handle technical jargon.
- The authors should discuss the computational efficiency of the proposed algorithms and how they scale with dataset size.
- If applicable, the authors should discuss possible limitations of their approach to address problems of privacy and fairness.
- While the authors might fear that complete honesty about limitations might be used by reviewers as grounds for rejection, a worse outcome might be that reviewers discover limitations that aren't acknowledged in the paper. The authors should use their best judgment and recognize that individual actions in favor of transparency play an important role in developing norms that preserve the integrity of the community. Reviewers will be specifically instructed to not penalize honesty concerning limitations.

### 3. Theory assumptions and proofs

Question: For each theoretical result, does the paper provide the full set of assumptions and a complete (and correct) proof?

Answer: [NA]

Justification: This paper does not include theoretical results.

Guidelines:

- The answer NA means that the paper does not include theoretical results.
- All the theorems, formulas, and proofs in the paper should be numbered and cross-referenced.
- All assumptions should be clearly stated or referenced in the statement of any theorems.
- The proofs can either appear in the main paper or the supplemental material, but if they appear in the supplemental material, the authors are encouraged to provide a short proof sketch to provide intuition.
- Inversely, any informal proof provided in the core of the paper should be complemented by formal proofs provided in appendix or supplemental material.
- Theorems and Lemmas that the proof relies upon should be properly referenced.

#### 4. Experimental result reproducibility

Question: Does the paper fully disclose all the information needed to reproduce the main experimental results of the paper to the extent that it affects the main claims and/or conclusions of the paper (regardless of whether the code and data are provided or not)?

Answer: [Yes]

Justification: We provide a comprehensive description of our crystal generation framework in §3, comprising a LLMs-based constraint generator and a diffusion-based structure generator. In §4, we detail the datasets, the experimental process for obtaining results, along with required Python Class and parameter configurations. In Appendix B.1, we document the model hyper-parameters and hardware specifications used during training.

Guidelines:

- The answer NA means that the paper does not include experiments.
- If the paper includes experiments, a No answer to this question will not be perceived well by the reviewers: Making the paper reproducible is important, regardless of whether the code and data are provided or not.
- If the contribution is a dataset and/or model, the authors should describe the steps taken to make their results reproducible or verifiable.
- Depending on the contribution, reproducibility can be accomplished in various ways. For example, if the contribution is a novel architecture, describing the architecture fully might suffice, or if the contribution is a specific model and empirical evaluation, it may be necessary to either make it possible for others to replicate the model with the same dataset, or provide access to the model. In general, releasing code and data is often one good way to accomplish this, but reproducibility can also be provided via detailed instructions for how to replicate the results, access to a hosted model (e.g., in the case of a large language model), releasing of a model checkpoint, or other means that are appropriate to the research performed.
- While NeurIPS does not require releasing code, the conference does require all submissions to provide some reasonable avenue for reproducibility, which may depend on the nature of the contribution. For example
  - (a) If the contribution is primarily a new algorithm, the paper should make it clear how to reproduce that algorithm.
  - (b) If the contribution is primarily a new model architecture, the paper should describe the architecture clearly and fully.
  - (c) If the contribution is a new model (e.g., a large language model), then there should either be a way to access this model for reproducing the results or a way to reproduce the model (e.g., with an open-source dataset or instructions for how to construct the dataset).

- (d) We recognize that reproducibility may be tricky in some cases, in which case authors are welcome to describe the particular way they provide for reproducibility. In the case of closed-source models, it may be that access to the model is limited in some way (e.g., to registered users), but it should be possible for other researchers to have some path to reproducing or verifying the results.

## 5. Open access to data and code

Question: Does the paper provide open access to the data and code, with sufficient instructions to faithfully reproduce the main experimental results, as described in supplemental material?

Answer: [Yes]

Justification: We follow the NeurIPS code and data submission guidelines, and provide the datasets used in this paper, the URL to access the model code, model weights, and inference scripts in the supplementary materials.

Guidelines:

- The answer NA means that paper does not include experiments requiring code.
- Please see the NeurIPS code and data submission guidelines (<https://nips.cc/public/guides/CodeSubmissionPolicy>) for more details.
- While we encourage the release of code and data, we understand that this might not be possible, so “No” is an acceptable answer. Papers cannot be rejected simply for not including code, unless this is central to the contribution (e.g., for a new open-source benchmark).
- The instructions should contain the exact command and environment needed to run to reproduce the results. See the NeurIPS code and data submission guidelines (<https://nips.cc/public/guides/CodeSubmissionPolicy>) for more details.
- The authors should provide instructions on data access and preparation, including how to access the raw data, preprocessed data, intermediate data, and generated data, etc.
- The authors should provide scripts to reproduce all experimental results for the new proposed method and baselines. If only a subset of experiments are reproducible, they should state which ones are omitted from the script and why.
- At submission time, to preserve anonymity, the authors should release anonymized versions (if applicable).
- Providing as much information as possible in supplemental material (appended to the paper) is recommended, but including URLs to data and code is permitted.

## 6. Experimental setting/details

Question: Does the paper specify all the training and test details (e.g., data splits, hyper-parameters, how they were chosen, type of optimizer, etc.) necessary to understand the results?

Answer: [Yes]

Justification: In §4.2 and Appendix B.1, we provide detailed descriptions of dataset splits, along with the hyper-parameters configurations and optimizer types employed during model training.

Guidelines:

- The answer NA means that the paper does not include experiments.
- The experimental setting should be presented in the core of the paper to a level of detail that is necessary to appreciate the results and make sense of them.
- The full details can be provided either with the code, in appendix, or as supplemental material.

## 7. Experiment statistical significance

Question: Does the paper report error bars suitably and correctly defined or other appropriate information about the statistical significance of the experiments?

Answer: [Yes]

Justification: We describe the statistical methods for symmetry precision in Appendix B.2, present the calculation methods of the matching rate and RMSE in crystal structure generation in §4.2, and introduce the absolute error probability distribution and RMSE computation in property error evaluation in §4.3.

Guidelines:

- The answer NA means that the paper does not include experiments.
- The authors should answer "Yes" if the results are accompanied by error bars, confidence intervals, or statistical significance tests, at least for the experiments that support the main claims of the paper.
- The factors of variability that the error bars are capturing should be clearly stated (for example, train/test split, initialization, random drawing of some parameter, or overall run with given experimental conditions).
- The method for calculating the error bars should be explained (closed form formula, call to a library function, bootstrap, etc.)
- The assumptions made should be given (e.g., Normally distributed errors).
- It should be clear whether the error bar is the standard deviation or the standard error of the mean.
- It is OK to report 1-sigma error bars, but one should state it. The authors should preferably report a 2-sigma error bar than state that they have a 96% CI, if the hypothesis of Normality of errors is not verified.
- For asymmetric distributions, the authors should be careful not to show in tables or figures symmetric error bars that would yield results that are out of range (e.g. negative error rates).
- If error bars are reported in tables or plots, The authors should explain in the text how they were calculated and reference the corresponding figures or tables in the text.

## 8. Experiments compute resources

Question: For each experiment, does the paper provide sufficient information on the computer resources (type of compute workers, memory, time of execution) needed to reproduce the experiments?

Answer: [Yes]

Justification: In Appendix B.4, we detail the computational resources consumed during the experiments, including compute workers, memory allocation, and execution time.

Guidelines:

- The answer NA means that the paper does not include experiments.
- The paper should indicate the type of compute workers CPU or GPU, internal cluster, or cloud provider, including relevant memory and storage.
- The paper should provide the amount of compute required for each of the individual experimental runs as well as estimate the total compute.
- The paper should disclose whether the full research project required more compute than the experiments reported in the paper (e.g., preliminary or failed experiments that didn't make it into the paper).

## 9. Code of ethics

Question: Does the research conducted in the paper conform, in every respect, with the NeurIPS Code of Ethics <https://neurips.cc/public/EthicsGuidelines?>

Answer: [Yes]

Justification: We have thoroughly read and understood the NeurIPS Code of Ethics, and affirm that the research presented in this paper complies with the NeurIPS Code of Ethics in all aspects.

Guidelines:

- The answer NA means that the authors have not reviewed the NeurIPS Code of Ethics.
- If the authors answer No, they should explain the special circumstances that require a deviation from the Code of Ethics.

- The authors should make sure to preserve anonymity (e.g., if there is a special consideration due to laws or regulations in their jurisdiction).

#### 10. **Broader impacts**

Question: Does the paper discuss both potential positive societal impacts and negative societal impacts of the work performed?

Answer: [Yes]

Justification: In Appendix D, we discuss both the positive and negative societal impacts of the proposed crystal structure generation framework.

Guidelines:

- The answer NA means that there is no societal impact of the work performed.
- If the authors answer NA or No, they should explain why their work has no societal impact or why the paper does not address societal impact.
- Examples of negative societal impacts include potential malicious or unintended uses (e.g., disinformation, generating fake profiles, surveillance), fairness considerations (e.g., deployment of technologies that could make decisions that unfairly impact specific groups), privacy considerations, and security considerations.
- The conference expects that many papers will be foundational research and not tied to particular applications, let alone deployments. However, if there is a direct path to any negative applications, the authors should point it out. For example, it is legitimate to point out that an improvement in the quality of generative models could be used to generate deepfakes for disinformation. On the other hand, it is not needed to point out that a generic algorithm for optimizing neural networks could enable people to train models that generate Deepfakes faster.
- The authors should consider possible harms that could arise when the technology is being used as intended and functioning correctly, harms that could arise when the technology is being used as intended but gives incorrect results, and harms following from (intentional or unintentional) misuse of the technology.
- If there are negative societal impacts, the authors could also discuss possible mitigation strategies (e.g., gated release of models, providing defenses in addition to attacks, mechanisms for monitoring misuse, mechanisms to monitor how a system learns from feedback over time, improving the efficiency and accessibility of ML).

#### 11. **Safeguards**

Question: Does the paper describe safeguards that have been put in place for responsible release of data or models that have a high risk for misuse (e.g., pretrained language models, image generators, or scraped datasets)?

Answer: [NA]

Justification: Our data are exclusively sourced from open-source, risk-free crystal structure datasets. Furthermore, this study does not involve any high-risk scenarios with potential for model misuse, such as large language model pre-training or image generation.

Guidelines:

- The answer NA means that the paper poses no such risks.
- Released models that have a high risk for misuse or dual-use should be released with necessary safeguards to allow for controlled use of the model, for example by requiring that users adhere to usage guidelines or restrictions to access the model or implementing safety filters.
- Datasets that have been scraped from the Internet could pose safety risks. The authors should describe how they avoided releasing unsafe images.
- We recognize that providing effective safeguards is challenging, and many papers do not require this, but we encourage authors to take this into account and make a best faith effort.

#### 12. **Licenses for existing assets**

Question: Are the creators or original owners of assets (e.g., code, data, models), used in the paper, properly credited and are the license and terms of use explicitly mentioned and properly respected?

Answer: [Yes]

Justification: We confirm that all assets used in the paper, including code, data, and models, have been properly credited, and the license and usage terms have been explicitly mentioned and complied with.

Guidelines:

- The answer NA means that the paper does not use existing assets.
- The authors should cite the original paper that produced the code package or dataset.
- The authors should state which version of the asset is used and, if possible, include a URL.
- The name of the license (e.g., CC-BY 4.0) should be included for each asset.
- For scraped data from a particular source (e.g., website), the copyright and terms of service of that source should be provided.
- If assets are released, the license, copyright information, and terms of use in the package should be provided. For popular datasets, [paperswithcode.com/datasets](https://paperswithcode.com/datasets) has curated licenses for some datasets. Their licensing guide can help determine the license of a dataset.
- For existing datasets that are re-packaged, both the original license and the license of the derived asset (if it has changed) should be provided.
- If this information is not available online, the authors are encouraged to reach out to the asset's creators.

### 13. New assets

Question: Are new assets introduced in the paper well documented and is the documentation provided alongside the assets?

Answer: [Yes]

Justification: We provide the assets introduced in this paper in the supplementary material, including the dataset, URLs to model code, model weights, inference scripts, and corresponding documentation.

Guidelines:

- The answer NA means that the paper does not release new assets.
- Researchers should communicate the details of the dataset/code/model as part of their submissions via structured templates. This includes details about training, license, limitations, etc.
- The paper should discuss whether and how consent was obtained from people whose asset is used.
- At submission time, remember to anonymize your assets (if applicable). You can either create an anonymized URL or include an anonymized zip file.

### 14. Crowdsourcing and research with human subjects

Question: For crowdsourcing experiments and research with human subjects, does the paper include the full text of instructions given to participants and screenshots, if applicable, as well as details about compensation (if any)?

Answer: [NA]

Justification: This paper focuses on crystal structure generation, and does not involve crowdsourcing nor research with human subjects.

Guidelines:

- The answer NA means that the paper does not involve crowdsourcing nor research with human subjects.
- Including this information in the supplemental material is fine, but if the main contribution of the paper involves human subjects, then as much detail as possible should be included in the main paper.
- According to the NeurIPS Code of Ethics, workers involved in data collection, curation, or other labor should be paid at least the minimum wage in the country of the data collector.

**15. Institutional review board (IRB) approvals or equivalent for research with human subjects**

Question: Does the paper describe potential risks incurred by study participants, whether such risks were disclosed to the subjects, and whether Institutional Review Board (IRB) approvals (or an equivalent approval/review based on the requirements of your country or institution) were obtained?

Answer: [NA]

Justification: This paper focuses on crystal structure generation, and does not involve crowdsourcing nor research with human subjects.

Guidelines:

- The answer NA means that the paper does not involve crowdsourcing nor research with human subjects.
- Depending on the country in which research is conducted, IRB approval (or equivalent) may be required for any human subjects research. If you obtained IRB approval, you should clearly state this in the paper.
- We recognize that the procedures for this may vary significantly between institutions and locations, and we expect authors to adhere to the NeurIPS Code of Ethics and the guidelines for their institution.
- For initial submissions, do not include any information that would break anonymity (if applicable), such as the institution conducting the review.

**16. Declaration of LLM usage**

Question: Does the paper describe the usage of LLMs if it is an important, original, or non-standard component of the core methods in this research? Note that if the LLM is used only for writing, editing, or formatting purposes and does not impact the core methodology, scientific rigor, or originality of the research, declaration is not required.

Answer: [Yes]

Justification: We have read and complied with the NeurIPS LLM Policy. Specifically, we elaborate on the usage of LLMs in §3.2, detail the tools and parameters for fine-tuning LLMs in Appendix B.1, and present the testing results of the LLMs in §3.2.

Guidelines:

- The answer NA means that the core method development in this research does not involve LLMs as any important, original, or non-standard components.
- Please refer to our LLM policy (<https://neurips.cc/Conferences/2025/LLM>) for what should or should not be described.

## **Supplementary Material**

In the supplementary materials, we provide the data, source code, weight files, scripts, and partial experimental results used in this work. Specifically, the CrystalGF file contains the source code, code environment, yaml files, scripts, and some experimental results of our proposed method. Pretrained model and lora weights can be downloaded at <https://modelscope.cn/models/chachapro/CrystalGF>. Data and code can be found at <https://github.com/chachapro/CrystalGF>. For Con-CDVAE and Matter-Gen, we provide the training results used for the experimental comparisons in this paper. Meanwhile, we have ensured that all content within the supplementary materials and website links has been anonymized.